

# Numerical Relativity Injection Infrastructure

Patricia Schmidt,<sup>1,2</sup> Ian W. Harry,<sup>3</sup> and Harald P. Pfeiffer<sup>3,4</sup>

<sup>1</sup>*LIGO Laboratory, California Institute of Technology, MS 100-36, Pasadena, California 91125, USA*

<sup>2</sup>*Theoretical Astrophysics, Walter Burke Institute for Theoretical Physics, California Institute of Technology, Pasadena, California 91125, USA*

<sup>3</sup>*Max Planck Institute for Gravitational Physics (Albert-Einstein-Institute), Am Mühlenberg 1, Potsdam-Golm, 14476, Germany*

<sup>4</sup>*Canadian Institute for Theoretical Astrophysics, 60 St. George Street, University of Toronto, Toronto, ON M5S 3H8, Canada*

(Dated: May 4, 2016)

This document describes the new standardised NR injection infrastructure in the LIGO Algorithms Library (LAL), which henceforth allows for the usage of Numerical Relativity (NR) waveforms as a discrete waveform approximant in LAL. With this new interface, NR waveforms provided in the appropriate format can directly be used as mock GW signals (“injections”) for LIGO data analyses, which include parameter estimation, searches, hardware injections etc. The interface handles higher-order modes making them directly accessible to LIGO data analyses for the very first time. The NR injection infrastructure also takes care of waveform frame conventions and transforms the NR data into the correct LAL frame.

## I. INTRODUCTION

Recently, LIGO has reported the first detection of gravitational waves (GW) from a merging binary black hole system [1]. Such coalescing compact binaries are prime sources for the ground-based interferometric GW detectors and play a critical role in LIGO data analysis. Whilst for low-mass systems only the early part of the binary evolution, the inspiral, is accessible to LIGO, for high-mass systems also the later stages, in particular the merger and ringdown of the final black, are visible in LIGO’s sensitivity band.

During the early part of the binary coalescence, the emitted gravitational waveforms are accurately described by an analytic post-Newtonian expansion of the Einstein field equations [2]. To obtain the waveforms for the final stages, the full non-linear solutions of the field equations are required, which are provided by Numerical Relativity (NR) (see for example [3] for an overview). Regarding the usage of NR waveforms for LIGO data analysis, so far, NR merger waveforms have predominantly been used to calibrate the merger-ringdown section of analytic waveform models which describe the complete inspiral-merger-ringdown (IMR) signal [4, 5], to test such models against independent NR waveforms not used in the construction and to determine the physical properties of the remnant black hole [6].

In the Advanced detector era, however, we want to be able to directly use NR waveforms in gravitational-wave searches and parameter estimation, to test General Relativity and to assess the systematics of analytic waveform models within a uniform framework. This is now possible with the recently implemented simple infrastructure, which allows for the treatment of NR waveforms as a “discrete” waveform approximant provided the NR data are available in a *specific format*.

In previous efforts, BBH hybrid waveforms constructed by combining a PN inspiral with an NR merger-ringdown waveform, have been used in LIGO data analysis and parameter estimation in the NINJA and NINJA-2 projects [7, 8]. These hybrids only contained the dominant harmonics, the  $(\ell, |m|) = (2, 2)$  modes, and required the NR waveforms to be linearly interpolated and resampled at uniform times for a given sampling rate  $f_s$ . In the NINJA framework, the resampling was performed *before* inserting the total mass scale, resulting in very memory-intensive operations, since the finest  $\Delta t$  for a given  $f_s$  is determined by the highest total mass one wants to be able to resolve.

The new infrastructure handles this differently, in the following way: Firstly, since it naturally handles higher-order modes, it uses a highly compressed data format to represent the NR data to reduce the storage requirements and reduce I/O time. Secondly, the compressed NR data are interpolated using 1D spline interpolation, and the resulting interpolants are evaluated *after* the mass scale has been inserted. This avoids high-memory operations and also bypasses the need to store unnecessarily large data files. The new injection infrastructure fully implemented in LAL and supersedes any previously used NR modules.

The remainder of this technical document is organised as follows: In Sec. II we provide a brief summary of the NR data format and metadata required as input. In Sec. III we describe the basics of the waveform generation code and give explicit examples of how the NR waveforms are evaluated in lalsimulation/pycbc. Sec. IV details the frame transformations between the NR simulation frame and the LAL wave frame. We highlight caveats and desired future improvements in Sec. V.

## II. WAVEFORM FORMAT

In Numerical Relativity one solves for the complete space-time of the binary system. For data analysis purposes however, one requires the gravitational-wave strain  $h(t)$  far from the source. The relevant numerical quantity is the metric perturbation  $h_{ij}^{TT}$  as computed in the transverse-traceless gauge (TT).

There are different way of computing the metric perturbation from a numerical evolution. The most common methods include the use of the complex Weyl scalar  $\Psi_4$ , which is related to the metric perturbation via two time derivatives, or the Regge-Wheeler-Zerilli formalism computes the metric perturbation in the wave-zone as a perturbation of the Schwarzschild spacetime.

In the TT gauge, the metric perturbation has two independent real polarisations,  $h_+$  and  $h_\times$ , which can be written as a complex strain by

$$h = h_+ - ih_\times \in \mathbb{C}, \quad (1)$$

where  $h_+, h_\times \in \mathbb{R}$ .

Let  $(t, x, y, z)$  be a Cartesian coordinate system in the wave-zone, which is related to the polar coordinates  $(r, \theta, \phi)$  by the standard means. In this coordinate system, the metric perturbation is commonly decomposed into *modes* in a basis of spin-weighted spherical harmonics,  ${}^{-2}Y_{\ell m}$ , of spin weight  $s = -2$ , where the GW propagation direction is the radial unit vector  $\mathbf{r}$ . For any point  $(\theta, \phi)$  on the unit sphere, the GW strain can then be shown to take the following form:

$$h^{\text{NR}}(t; \theta, \phi) = h_+^{\text{NR}} - ih_\times^{\text{NR}} = \sum_{\ell=2}^{\infty} \sum_{m=-\ell}^{\ell} H_{\ell m}(t) {}^{-2}Y_{\ell m}(\theta, \phi). \quad (2)$$

As for any wave, we can also write each NR gravitational-wave mode  $H_{\ell m}$  as an amplitude  $A_{\ell m}$  and a phase  $\Phi_{\ell m}$ ,

$$H_{\ell m}(t) = A_{\ell m}(t) e^{i\Phi_{\ell m}(t)}. \quad (3)$$

The amplitude of each mode is its complex norm, the phase is the unwrapped argument of the complex time series  $h_{\ell m}$ .

### A. Spline Compression

Gravitational waveforms for LIGO data analysis purposes require uniform sampling in time for a given sampling frequency  $f_s$ . NR datasets however, are commonly not uniformly sampled and if they are, the sampling interval  $dt$  may not necessarily correspond to the one required by data analysis tools. It is therefore unavoidable to interpolate the NR data such that for any total mass  $M$  and sampling rate the NR waveforms can be resampled accordingly. Whilst the NR data could simply be interpolated as they are, we choose to reduce the data by performing 1D spline compression on the NR data [9]. This is a particular advantage for long simulations or hybrid PN-NR data, but also significantly reduces the storage and I/O for pure NR data. It is mandatory that the NR data files are provided in the correct compressed file format, which is as follows:

The 1D spline compression is performed separately for each mode amplitude  $A_{\ell m}$  and phase  $\Phi_{\ell m}$ . The compression is achieved by applying a greedy algorithm to the NR data, which selects the near-optimal points to construct a univariate spline interpolant with a specified global accuracy. By default, the interpolants are constructed using fifth degree polynomials and a tolerance of  $10^{-6}$ , i.e. if the spline is evaluated at the discrete times  $t_i$  of the NR data, the original NR values are recovered with an error smaller than the specified tolerance. For a detailed description of this method and the accuracy of the obtained interpolants, we refer the reader to [9]. The spline compression is performed using the publicly available python package “romSpline” by Chad R. Galley [10].

The spline interpolants for each amplitude and phase are obtained via `romSpline.ReducedOrderSpline()` as follows:

```
import romSpline
spline = romSpline.ReducedOrderSpline(time_data, amplitude / phase_data, verbose=False)
spline.write('filename.h5')
```

Note: a newer version of romSpline now also allows to pass a group descriptor, i.e. writing to file as intermediate step may be avoided.

Once the spline interpolants have been obtained, they have to be stored as individual groups in a *single HDF5 file* with the following mandatory group naming conventions:

- Amplitude group: **amp.l#1\_m#2**

- Phase group: **phase\_l#1\_m#2**,

where (#1, #2) are placeholders for  $(\ell, m)$ , e.g., for  $(\ell = 2, m = -2)$  the naming convention is `phase_l2_m-2` and `amp_l2_m-2`.

Pure NR data without a hybridised PN inspiral need to have the initial *junk radiation* removed before the spline interpolants are constructed but no tapering should be applied at the beginning or end of the waveform data. Following the LAL waveform convention, the waveforms also need to be aligned such that the peak of the waveform occurs at  $t_{\text{peak}} = 0$  before constructing the interpolants. In addition to the amplitude and phase groups, we highly recommend to also include the NR times as a group in the HDF5 file.

## B. Metadata

The metadata format is adapted from the original NINJA-2 metadata format [11], and whilst then metadata were stored an additional text file, it is now mandatory that each HDF5 contains a *minimal* set of metadata stored as *attributes* of the HDF5 file. If a metadata text file exists, however, we recommend that it is additionally included in the HDF5 file.

In the current implementation, the required metadata which are time-dependent (see list below) have to contain the values associated with the first entry in the stored time series. For pure NR data, since the junk radiation has to be removed, these are *not* the initial data of the simulation. We refer to this very first data point stored in the HDF5 file as the *beginning* of the waveform data. Source frame dependent metadata should be given in the NR simulation frame.

The required metadata attributes are the following:

- ['NR-group']: string to identify the NR group/code
- ['type']: keyword description of the simulation. Allowed values are: aligned-spins, non spinning, precessing.
- ['name']: alternative simulation name or internal simulation identifier
- ['object1']: keyword description to identify the object type. Allowed values are: BH, NS
- ['object2']: keyword description to identify the object type. Allowed values are: BH, NS
- ['mass1']: mass of the heavier object
- ['mass2']: mass of the lighter object
- ['eta']: the symmetric mass ratio of the simulation
- ['spin1x']: x-component of the dimensionless spin of the heavier object
- ['spin1y']: y-component of the dimensionless spin of the heavier object
- ['spin1z']: z-component of the dimensionless spin of the heavier object
- ['spin2x']: x-component of the dimensionless spin of the lighter object
- ['spin2y']: y-component of the dimensionless spin of the lighter object
- ['spin2z']: z-component of the dimensionless spin of the lighter object
- ['LNhatx']: x-component of the orbital angular momentum unit vector
- ['LNhaty']: y-component of the orbital angular momentum unit vector
- ['LNhatz']: z-component of the orbital angular momentum unit vector
- ['nhatx']: x-component of the orbital separation unit vector
- ['nhaty']: y-component of the orbital separation unit vector
- ['nhatz']: z-component of the orbital separation unit vector
- ['f\_lower\_at\_1MSUN']: frequency of the (2,2)-mode in Hz at the beginning of the waveform scaled to 1 solar mass

To reduce potential ambiguities, we further recommend adding the following additional metadata:

- [eccentricity]: eccentricity parameter of the simulation
- [PN\_approximant]: string identifier for the inspiral if hybrid data are stored

### III. NR WAVEFORM EVALUATION IN LAL

Once the HDF5 file has been provided, the NR waveforms can be evaluated through the standard waveform interfaces `ChooseTDWaveform()` in LAL and `get_td_waveform()` in pyCBC [12]. The approximant name is “NR\_hdf5”. The spline data are read from file and evaluated for the desired extrinsic parameters. The intrinsic parameters in NR simulations are fixed, internal checks on the mass ratio and the spin components are performed to guarantee the consistency between the values passed in the waveform generation call and metadata values. The waveform generator requires the input spin values to be defined as given in Eqn. (46). In general, these are different to the values of the spin metadata and need to be computed using the metadata for the spins, the orbital angular momentum and the orbital separation.

For a given starting frequency and total mass, a time array is allocated based on an estimate of the waveform length. We use the LAL function `SimIMRSEOBNRv2ChirpTimeSingleSpin()` to estimate the waveform length with an additional leverage of 10%. If the NR waveforms are not long enough for a given total mass and starting frequency, the generation is aborted. From the estimated length and the desired sampling rate, the discrete time series for the spline evaluation is determined.

To construct the NR GW polarisations  $h_+^{\text{NR}}$  and  $h_\times^{\text{NR}}$ , the splines for each amplitude and phase are evaluated at the points of the discrete time times, weighted by the  ${}^{-2}Y_{\ell m}$ , and summed up accordingly:

$$\text{Re}(H_{\ell m}) = A_{\ell m} \cos(\Phi_{\ell m}), \quad (4)$$

$$\text{Im}(H_{\ell m}) = A_{\ell m} \sin(\Phi_{\ell m}), \quad (5)$$

$$h_+^{\text{NR}} = \sum_{\ell, m} \text{Re}(H_{\ell m}) \text{Re}({}^{-2}Y_{\ell m}) - \text{Im}(H_{\ell m}) \text{Im}({}^{-2}Y_{\ell m}), \quad (6)$$

$$h_\times^{\text{NR}} = \sum_{\ell, m} -\text{Re}(H_{\ell m}) \text{Im}({}^{-2}Y_{\ell m}) - \text{Im}(H_{\ell m}) \text{Re}({}^{-2}Y_{\ell m}). \quad (7)$$

Note that all waveform modes  $(\ell, m)$  present in the HDF5 file are used to compute the two polarisations. The algorithm will incorporate any mode between  $\ell = 2$  and  $\ell = 8$  if present in the HDF5 file but at least the  $(\ell = 2, m = 2)$  has to be present in the NR data file.

The compressed NR data files do not store the splines themselves, but the knots, errors, the polynomial degree etc. In the pyCBC implementation, the splines are constructed from the HDF5 file via the python function `UnivariateSpline`, in the LAL implementation regular GSL interpolation is performed. Fig. 1 shows an example comparison between NR waveforms obtained using the pyCBC and the LAL waveform generators. The mismatch between the waveforms is less than  $10^{-7}$ . This is consistent with the level of disagreement expected due to the different numerical interpolation routines.

The source code can be found in

```
lalsuite / lalsimulation / src / LALSimIMRNRWaveforms.c
```

#### A. Examples

There are a variety of different ways to generate waveforms using LIGO data analysis software. Here, we give two explicit examples for function calls in python: The first example uses the pyCBC implementation, the second one uses the SWIG-wrapped version of lalsimulation.

1. Using the pyCBC waveform interface `get_td_waveform()` :

```
from pycbc.waveform import get_td_waveform

hp, hc = get_td_waveform(approximant='NR_hdf5',
```

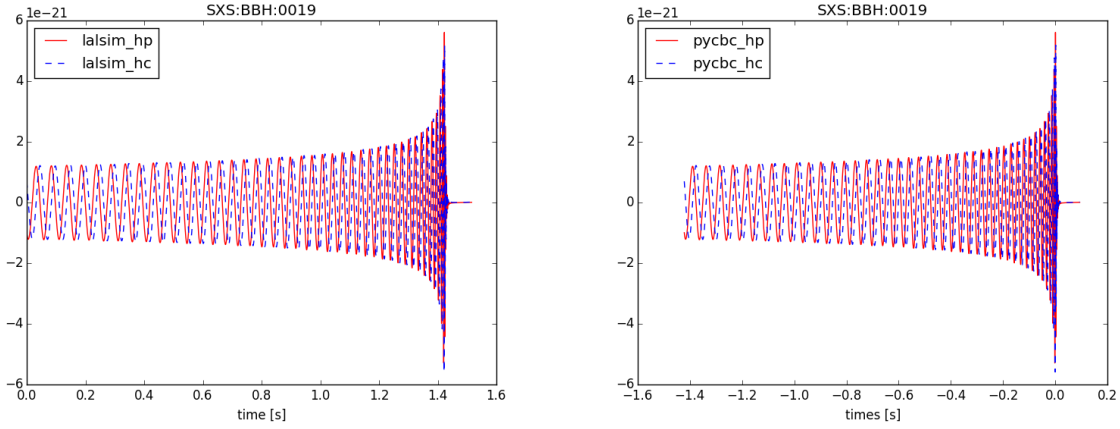


FIG. 1: Those need to be replaced with updated version. The waveform polarizations  $h_+$  (solid, red) and  $h_\times$  (dashed, blue) of the publicly available SXS waveform SXS:BBH:0019 generated via the waveform interface in lalsimulation (left panel) and in pyCBC (right panel).

```

numrel_data = '/PATH/TO/HDF5',
mass1, mass2,
spin1x, spin1y, spin1z,
spin2x, spin2y, spin2z,
delta_t, f_lower, f_ref,
inclination, distance,
coa_phase)

```

2. Using the implementation in lalsimulation through SWIG:

```

import lalsimulation as lalsim

flags = lalsim.SimInspiralCreateWaveformFlags()

lalsim.SimInspiralSetNumrelData(flags, '/PATH/TO/HDF5')

hp, hc = lalsim.SimInspiralChooseTDWaveform(phiRef,
      deltaT, m1 * MSUN_SI, m2 * MSUN_SI,
      s1x, s1y, s1z,
      s2x, s2y, s2z,
      fStart, fRef,
      distance, inclination,
      lambda_1 = 0, lambda_2 = 0,
      flags, nonGRparams=None,
      amplitudeO=-1, phaseO=-1,
      approximant=lalsim.NR_hdf5),

```

where  $\lambda_1$  denote the tidal deformation parameters, which vanish in the case of black holes.

Fig. 1 shows the two waveform polarizations  $h_+$  and  $h_\times$  for the binary black hole case simulated in case SXS:BBH:0019 from the publicly available SXS catalogue [13] for a total mass of  $50 M_\odot$ . The dimensionless spins for this simulation are  $\vec{\chi}_1 = (0, 0, -0.5)$  and  $\vec{\chi}_2 = (0, 0, 0.499)$  and the component masses are  $m_1 = 30.01360$  and  $m_2 = 20.00954$ . As extrinsic parameters, we choose the following: distance=100Mpc, inclination=0.4rad, deltaT=1.0/16384, fStart=fRef=18.88Hz. We do not alter the reference phase but instead pass the metadata value stored in the HDF5 file. We have obtained those polarizations via the lalsimulation interface and also via the test verification code in pycbc. The match between the waveforms obtained from the two numerical implementations is  $\mathcal{M} = 0.999999999341$ .

## IV. LAL COORDINATE FRAMES FOR PRECESSING BINARIES AND NR INJECTIONS

### 1. Executive summary: changes of conventions

In recent discussions, it became apparent that current LAL conventions to specify precessing binary compact objects are deficient: (i) The phase-angle  $\text{phiRef}$  couples specification of the line-of-sight to Earth with specification of spin components  $S_{1x}$ ,  $S_{1y}$ ,  $S_{1z}$ ,  $S_{2x}$ ,  $S_{2y}$ ,  $S_{2z}$ . To compute waveforms for the *identical* CBC system viewed from different directions, one may have to specify different values for the in-plane spin-components  $S_{1x}$ ,  $S_{1y}$ ,  $S_{2x}$ ,  $S_{2y}$ . (ii) Several existing waveform models do not conform to the current LAL convention, already implementing the improvements suggested in this note.

Concretely, it is suggested to specify spin-components in a geometric way based on the angular momentum  $\hat{L}$  and line connecting body 2 to body 1,  $\hat{n}$ :

$$S_{1x} \stackrel{\text{ref}}{=} \vec{\chi}_1 \cdot \hat{n}, \quad (8)$$

$$S_{1y} \stackrel{\text{ref}}{=} \vec{\chi}_1 \cdot (\hat{L} \times \hat{n}), \quad (9)$$

$$S_{1z} \stackrel{\text{ref}}{=} \vec{\chi}_1 \cdot \hat{L}, \quad (10)$$

(and similarly for the second body). The symbol  $\stackrel{\text{ref}}{=}$  indicates that equality only holds at the reference time, as spins generically precess during an inspiral.

Furthermore, it is suggested to specify orientation of eccentric orbits through the angles

$$\text{phiRef} = \Phi \stackrel{\text{ref}}{=} \angle(\hat{n}, \text{line-of-ascending-node}), \quad (11)$$

$$\text{mean\_anomaly} = \delta. \quad (12)$$

### 2. Motivation & benefits of new conventions

Quite generally waveform modeling requires at least two coordinate systems, a “source-frame” in which it is convenient to specify properties of the source of gravitational waves, and a “wave-frame” which is adopted to wave-propagation to detectors on Earth. Furthermore, numerical relativity data is specified in whatever coordinates are employed during the numerical evolution, generally resulting in a third coordinate system.

This note defines coordinate frames for use in LAL. Specifically, we achieve:

1. Identification of a set of intrinsic parameters that fully describe the dynamics of a binary on an eccentric orbit, defined solely in terms of the source-frame (i.e. independent of the wave-frame).
2. Identification of three angles that describe the transformation between source- and wave-frame, which are independent of the intrinsic parameters.
3. Identification of parameters describing the orbital phase and periaapse location, which have a convenient circular-orbit limit: As the eccentricity tends to zero, one of the two phase-parameters reduces to the standard orbital phase for circular orbits, whereas the other becomes irrelevant.
4. Identities that relate the basis-vectors in the source-frame to the wave-frame (and vice versa). These identities are written in vectorial form and are valid in any coordinate system.

The orthogonal decomposition into intrinsic and extrinsic parameters (points 1 and 2) allows to change the direction at which a binary is viewed (i.e. the wave-frame), without having to adjust the parameters that determine the intrinsic dynamics. Point 3 prepares the ground for easy extension to eccentric waveforms. Point 4 is of particular relevance when translating NR data into LAL-conventions: Evaluating the vector identities in the NR-coordinate system, yields immediately the relation between NR coordinates and wave-frame.

### 3. NR waveform injections

NR data is assumed to be supplied in the data-format defined in [11], and so it needs to be transformed into the LAL wave-frame. For a given reference time, an entire NR data-set could in principle be transformed into the LAL frame by suitable

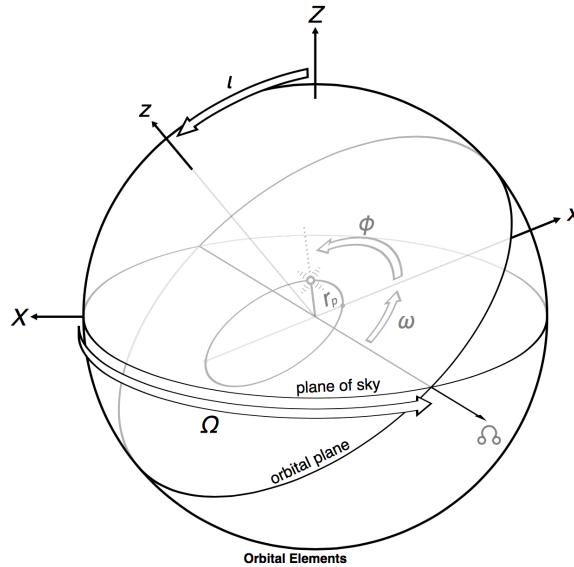


FIG. 2: Previous LAL coordinate frames. This diagram needs to be replaced by a new one, with the following changes: The  $x$ -axis should point along the line connecting the origin with body 1. The main-text  $\Phi$  is the angle between line of ascending node and  $\hat{n}$ , i.e. the sum of the picture  $\Phi + \omega$ . The mean-anomaly  $\delta$  in the main-text corresponds to the picture-symbol  $\Phi$ . For the recommended default  $\Omega = \pi/2$ , the line of ascending nodes agrees with  $\hat{Y}$  i.e. the rotation by the inclination angle  $i$  is about the  $\hat{Y}$ -axis.

transformations of each  $H_{\ell m}$ -mode. Applying such a rotation on the NR-data as a one-time pre-processing step before using it for injections suffers from two disadvantages:

First, the person who prepares the NR-data for LAL-use must perform the rotation, and must do so correctly. Since NR data is prepared separately by several NR groups, this opens the possibility of introducing errors in this step. Second, for precessing systems, the orbital angular momentum  $\hat{L}$  precesses. Therefore, pre-rotating the NR-data locks in the reference point, and one would need to generate a new pre-rotated NR-data for a different reference point. Since NR data is in geometric units, the NR-data would have to be separately rotated whenever the total mass of an injection changes.

To avoid both disadvantages, it is proposed to leave the NR-data in its original frame. Instead, the transformations between the LAL-convention and the NR-data are applied *at use* during the call to `ChooseTDwaveform`.

This note develops the necessary transformations to implement this technique. No assumptions are made on the NR-coordinate system, in order to allow for precession when NR-orbital angular momentum is typically *not* along the  $z$ -axis of the NR-coordinate system. The derived formulae also allow to choose an arbitrary reference point for the NR waveform, as long as orbital angular momentum and vector connecting the two bodies are known at that point.

#### 4. Outline

The rest of this note is organized as follows. Section IV A defines NR-frame, source-frame and wave-frame. Section IV B collects formulae to convert from one frame to another.

##### A. Frames

The frames defined here differ somewhat from the preceding LAL conventions, as spelled out in [http://software.ligo.org/docs/lalsuite/lalsimulation/group\\_lalsimulation\\_inspiral.html](http://software.ligo.org/docs/lalsuite/lalsimulation/group_lalsimulation_inspiral.html). The differences are needed to achieve the separation between intrinsic and extrinsic parameters. In the old conventions, the orbital phase  $\phi$  was also used as part of the rotation parameters that define the rotation between source- and wave-frame. Therefore, to “look” at the same binary from different angles used to require a suitable change in the spin-components tangential to the orbital plane.

1. NR frame( $\hat{e}_x, \hat{e}_y, \hat{e}_z$ )

This is just a generic coordinate system, without any regards to the concrete binary motion. Generic coordinate systems occur in numerical relativity, where the coordinates are chosen through same gauge-conditions, and the binary is evolving from some initial data. At some later time therefore, the coordinates will not have any particular, controlled properties.

The Cartesian basis-vectors are denoted

$$\hat{e}_x, \hat{e}_y, \hat{e}_z. \quad (13)$$

From these, spherical basis-vectors can be computed as usual

$$\hat{r} = \cos \phi \sin \theta \hat{e}_x + \sin \phi \sin \theta \hat{e}_y + \cos \theta \hat{e}_z \quad (14a)$$

$$\hat{\theta} = \cos \phi \cos \theta \hat{e}_x + \sin \phi \cos \theta \hat{e}_y - \sin \theta \hat{e}_z \quad (14b)$$

$$\hat{\phi} = -\sin \phi \hat{e}_x + \cos \phi \hat{e}_y. \quad (14c)$$

NR data is assumed to be given in spherical-harmonic modes of the NR coordinates, as defined in the NINJA data-formats document [11]:

$$h_+^{\text{NR}}(t_{\text{GW}}) = \frac{1}{2} (\hat{\theta}_i \hat{\theta}_j - \hat{\phi}_i \hat{\phi}_j) h^{ij}(t_{\text{GW}}) \quad (15a)$$

$$h_{\times}^{\text{NR}}(t_{\text{GW}}) = \frac{1}{2} (\hat{\theta}_i \hat{\phi}_j + \hat{\phi}_i \hat{\theta}_j) h^{ij}(t_{\text{GW}}), \quad (15b)$$

and

$$\begin{aligned} & \sum_{\ell=2}^{\infty} \sum_{m=-\ell}^{\ell} H_{\ell m}(t_{\text{GW}}) {}^{-2}Y_{\ell m}(\theta, \phi) \\ &= \frac{r}{M} \left( h_+^{\text{NR}}(t_{\text{GW}}) - ih_{\times}^{\text{NR}}(t_{\text{GW}}) \right). \end{aligned} \quad (16)$$

Specifically, the data-files are assumed to contain a time-series of the  $H_{\ell m}(t_{\text{GW}})$  modes; given an emission direction  $(\theta, \phi)$ , Eq. (16) yields the GW modes  $h_+^{\text{NR}}(t_{\text{GW}})$  and  $h_{\times}^{\text{NR}}(t_{\text{GW}})$ , according to the convention Eqs. (15).

The gravitational wave data are given in a time-coordinate  $t_{\text{GW}}$  of observers at large distance.

Let us now turn to a description of the dynamics of the two bodies. Numerical relativity defines a variety of vectors, the combination of which defines the instantaneous state of the two bodies. These are: The dimensionless spin vectors of the two bodies,

$$\vec{\chi}_1(t), \vec{\chi}_2(t); \quad (17)$$

The direction from body 2 to body 1,

$$\hat{n}(t); \quad (18)$$

the direction of the orbital angular momentum,

$$\hat{L}(t). \quad (19)$$

We do **not** make any assumption about the relation of the NR-orbital angular momentum vector  $\hat{L}$  relative to the NR coordinates[15]. One can further define an orbital frequency

$$\vec{\Omega}(t) = \hat{n}(t) \times \frac{d\hat{n}(t)}{dt}. \quad (20)$$

Equations (17)–(20) are defined in the strong-field region near the black holes, and are given as a function of the time-coordinate  $t$  employed by the NR simulation in the strong field regime.

The time-coordinates  $t_{\text{GW}}$  and  $t$  are defined at different regions of the space-time (far-zone vs. near-zone). Sometimes it is desirable to relate these two time-coordinates to each other, e.g. to make a statement about the dynamical state of the binary at the time “when a certain GW-frequency is reached”. Any relation between  $t_{\text{GW}}$  and  $t$  is ambiguous. Often NR simulations employ an approximation of “retarded time”, i.e.

$$t_{\text{GW}} = t \Big|_{\text{retarded}}. \quad (21)$$



However, in a dynamical space-time with black holes, two difficulties arise: First, the horizons are causally disconnected from future null infinity, so there are no outgoing null-rays that connect the horizons to the wave-zone. Second, when integrating null-rays “slightly outside” the horizons, the time-delay to infinity will depend on precisely where the integration was started, as well as on the initial direction of the null-ray. Therefore, any relation between  $t_{\text{GW}}$  and  $t$  should be viewed as approximate. One should further assume that different NR groups may use different definitions of  $t_{\text{GW}}$  in the data they compute. For instance, SpEC reports GW-waveforms extracted at *finite-radius* in terms of the NR coordinate,  $t_{\text{GW}} = t$ , whereas extrapolated waveforms are reported using a retarded time-coordinate with a correction of the rate of flow of time, see Equations (7), (14a) and (14b) of Boyle & Mroue [14].

## 2. LAL Source-Frame $(\hat{x}, \hat{y}, \hat{z})$

The LAL source-frame  $(\hat{x}, \hat{y}, \hat{z})$  is defined as follows:

1. The  $\hat{z}$ -axis points along the orbital angular momentum of the binary,

$$\hat{z}^{\text{ref}} \equiv \hat{L}. \quad (22)$$

2. The  $\hat{x}$ -axis points along the vector  $\hat{n}$  pointing from the second to the first body,

$$\hat{x}^{\text{ref}} \equiv \hat{n}. \quad (23)$$

3. The third vector  $\hat{y} = \hat{z} \times \hat{x}$  completes the triad.

The symbol  $\overset{\text{ref}}{\equiv}$  indicates that the respective equation is only required at the reference epoch. The reference epoch can be unambiguously specified by a reference-time  $t_{\text{ref}}$ . One can also specify a reference *orbital* frequency  $\Omega_{\text{ref}}$ , and infer  $t_{\text{ref}}$  via Eq. (20),  $\Omega(t_{\text{ref}}) = \Omega_{\text{ref}}$ . If the reference epoch is desired to be specified in terms of a *gravitational wave*-frequency, then the gravitational wave time  $t_{\text{GW}}$  needs to be related to the time-coordinate of the black hole dynamics,  $t$ . As discussed in the context of Eq. (21), such an identification is ambiguous and holds only approximately.

Equations (22) and (23) define the source-frame at the reference epoch only. They are chosen such that the spin-components  $(S_{x1}, S_{y1}, S_{z1})$  and  $(S_{2x}, S_{2y}, S_{2z})$  have coordinate-invariant meaning:  $S_{x1}$  is the projection of  $\vec{\chi}_1$  onto  $\hat{n}$ ,  $S_{z1}$  is the projection of  $\vec{\chi}_1$  onto  $\hat{L}$ , etc.

The source-frame does not rotate as the binary evolves. Specifically, the rotation between source-frame and wave-frame described below is constant in time.

A different reference epoch would lead to a different source-frame, related by some rotation. If the reference epoch is shifted by a small amount (comparable to the orbital time-scale),  $\hat{x}$  and  $\hat{y}$  would rotate with the binary. On the precession time-scale  $\hat{z}$  would change.

The source frame has no deep intrinsic, geometric significance. It is merely a vehicle to describe the spin-projections onto intrinsic geometric directions, and the basis-vectors  $(\hat{x}, \hat{y}, \hat{z})$  will be convenient when writing down the transformation to the wave-frame.

## 3. Intrinsic parameters of a binary

Given a reference epoch, a binary is specified by the following ten numbers:

- Two masses  $m_1, m_2$ .
- Two spin-vectors  $\vec{\chi}_1, \vec{\chi}_2$ , specified through the projections of the spin-vectors onto  $\hat{L}, \hat{n}$  and the third basis-vector (at reference time).
- Eccentricity  $e$ .
- Mean anomaly  $\delta$ . The mean anomaly is defined in terms of the current time  $t$ , the time of last periapsis passage  $T_{\text{previous}}$ , and the time of next periapsis passage  $T_{\text{next}}$ :

$$\delta = 2\pi \frac{t - T_{\text{previous}}}{T_{\text{next}} - T_{\text{previous}}}. \quad (24)$$

Eccentricity should be defined somehow “near” the reference epoch. A precise definition (if possible at all) is left to the future. For low eccentricity orbits, there is a competition between radiation reaction driven inspiral (which results in a slightly negative average radial velocity), and the oscillatory radial motion due to eccentricity. For sufficiently small eccentricity, minima in separation may no longer exist. If mean anomaly is still needed despite the quite low eccentricity in such cases, one will have to define periapsis as minimum of separation compared to a fiducial smooth inspiral trajectory.

#### 4. Wave-Frame ( $\hat{X}, \hat{Y}, \hat{Z}$ )

The wave-frame is adopted to the direction of the observer (i.e. Earth), such that its  $\hat{Z}$ -axis points toward the observer.  $\hat{X}$  and  $\hat{Y}$  represent basis-vectors orthogonal to the line-of-sight, i.e. they span the plane of the sky.

The wave-frame is completely specified by three angles:

1. The angle  $\Phi$  between line of ascending node and  $\hat{n}$  (at the reference time). [In Fig. 2, this angle corresponds to  $\Phi + \omega$ ]
2. The inclination  $\iota$ , i.e. the angle between orbital angular momentum  $\hat{L} = \hat{z}$  and the line-of-sight  $\hat{Z}$ .
3. The angle  $\Omega$  between the  $\hat{X}$ -axis and the line of ascending node (at the reference time).

These three angles happen to be the Euler angles of the rotation from wave-frame to source-frame.

The gravitational wave modes are defined as

$$h_+^W = \frac{1}{2} (\hat{X}_i \hat{X}_j - \hat{Y}_i \hat{Y}_j) h^{ij}, \quad (25a)$$

$$h_\times^W = \frac{1}{2} (\hat{X}_i \hat{Y}_j + \hat{Y}_i \hat{X}_j) h^{ij}, \quad (25b)$$

where the superscript ‘W’ indicates the LAL wave-frame. The angle  $\Omega$  merely rotates the  $\hat{X}$  and  $\hat{Y}$ . By definition Eq. (25), this merely rotates the polatization of the GW modes, and so  $\Omega$  is fully degenerate with the GW polarization.

Note that the phase-angle  $\Phi$  is specified without regard to the location of periapse of the binary (this differs from the previous LAL convention). This new definition decouples the specification of periapse location and the specification of orbital phase, and avoids the ambiguity that would arise in the zero-eccentricity limit of definitions involving periapse. Indeed, for fixed  $\Phi$  and fixed  $\delta$ , as eccentricity approaches zero, the waveforms will approach the identical circular form, independent of the value of  $\delta$ .

## B. Relationship between frames

### 1. From source-frame to wave-frame

The relation between source-frame and wave-frame can be easily derived following the three rotations that rotate one into the other frame:

Beginning in the source-frame,  $\hat{x}, \hat{y}, \hat{z}$ , we first apply the rotation by  $\Phi$  around  $\hat{z}$ , which yields a frame with basis-vectors  $\hat{p}, \hat{q}, \hat{z}$ :

$$\hat{p} = \cos \Phi \hat{x} - \sin \Phi \hat{y}, \quad (26a)$$

$$\hat{q} = \sin \Phi \hat{x} + \cos \Phi \hat{y}, \quad (26b)$$

$$\hat{z} = \hat{z}. \quad (26c)$$

The inverse rotation is

$$\hat{x} = \cos \Phi \hat{p} + \sin \Phi \hat{q}, \quad (27a)$$

$$\hat{y} = -\sin \Phi \hat{p} + \cos \Phi \hat{q}, \quad (27b)$$

$$\hat{z} = \hat{z}. \quad (27c)$$

The vectors  $\hat{p}, \hat{q}$  form an ortho-normal basis of the  $\hat{x}$ - $\hat{y}$  plane, such that  $\hat{p}$  points in the direction of ascending node.

Next, we rotate around the line of ascending node by the inclination  $\iota$ , resulting in basis-vectors

$$\hat{P} = \hat{p}, \quad (28a)$$

$$\hat{Q} = \cos \iota \hat{q} - \sin \iota \hat{z}, \quad (28b)$$

$$\hat{Z} = \sin \iota \hat{q} + \cos \iota \hat{z}. \quad (28c)$$

$\hat{P}$  and  $\hat{Q}$  form an orthonormal basis of the  $\hat{X}$ - $\hat{Y}$  plane with  $\hat{P}$  pointing in the direction of ascending node. The inverse rotation is

$$\hat{p} = \hat{P}, \quad (29a)$$

$$\hat{q} = \cos \iota \hat{Q} + \sin \iota \hat{Z}, \quad (29b)$$

$$\hat{z} = -\sin \iota \hat{Q} + \cos \iota \hat{Z}. \quad (29c)$$

The final rotation rotates  $\hat{P}$  and  $\hat{Q}$  around  $\hat{Z}$  into  $\hat{X}$ ,  $\hat{Y}$ :

$$\hat{X} = \cos \Omega \hat{P} - \sin \Omega \hat{Q}, \quad (30a)$$

$$\hat{Y} = \sin \Omega \hat{P} + \cos \Omega \hat{Q}, \quad (30b)$$

$$\hat{Z} = \hat{Z}. \quad (30c)$$

The inverse rotation is

$$\hat{P} = \cos \Omega \hat{X} + \sin \Omega \hat{Y}, \quad (31a)$$

$$\hat{Q} = -\sin \Omega \hat{X} + \cos \Omega \hat{Y}, \quad (31b)$$

$$\hat{Z} = \hat{Z}. \quad (31c)$$

Substituting Eqs. (26), (28) and (30) into each other, one obtains the entire transformation:

$$\begin{aligned} \hat{X} &= (\cos \Omega \cos \Phi - \sin \Omega \cos \iota \sin \Phi) \hat{x} \\ &\quad + (-\cos \Omega \sin \Phi - \sin \Omega \cos \iota \cos \Phi) \hat{y} \\ &\quad + \sin \Omega \sin \iota \hat{z}, \end{aligned} \quad (32a)$$

$$\begin{aligned} \hat{Y} &= (\sin \Omega \cos \Phi + \cos \Omega \cos \iota \sin \Phi) \hat{x} \\ &\quad + (-\sin \Omega \sin \Phi + \cos \Omega \cos \iota \cos \Phi) \hat{y} \\ &\quad - \cos \Omega \sin \iota \hat{z}, \end{aligned} \quad (32b)$$

$$\hat{Z} = \sin \iota \sin \Phi \hat{x} + \sin \iota \cos \Phi \hat{y} + \cos \iota \hat{z}. \quad (32c)$$

The inverse transformation is obtained from Eqs. (27), (29) and (31):

$$\begin{aligned} \hat{x} &= (\cos \Omega \cos \Phi - \sin \Omega \cos \iota \sin \Phi) \hat{X} \\ &\quad + (\sin \Omega \cos \Phi + \cos \Omega \cos \iota \sin \Phi) \hat{Y} \\ &\quad + \sin \iota \sin \Phi \hat{Z}, \end{aligned} \quad (33a)$$

$$\begin{aligned} \hat{y} &= (-\cos \Omega \sin \Phi - \sin \Omega \cos \iota \cos \Phi) \hat{X} \\ &\quad + (-\sin \Omega \sin \Phi + \cos \Omega \cos \iota \cos \Phi) \hat{Y} \\ &\quad + \sin \iota \cos \Phi \hat{Z}, \end{aligned} \quad (33b)$$

$$\hat{z} = \sin \Omega \sin \iota \hat{X} - \cos \Omega \sin \iota \hat{Y} + \cos \iota \hat{Z}. \quad (33c)$$

Equation (33c) shows that  $\Omega$  determines the direction of  $\hat{L} = \hat{z}$  on the plane of the sky. For  $\Omega = 0$ ,  $\hat{L}$  lies in the  $\hat{Y}$ - $\hat{Z}$  plane, and for  $\Omega = \pi/2$ , it lies in the  $\hat{X}$ - $\hat{Z}$  plane.

This latter choice ( $\Omega = \pi/2$ ) is already respected by many LAL waveform models. Therefore, in the absence of a reason to do otherwise, all waveform models should default to  $\Omega = \pi/2$ .

With this recommended default  $\Omega = \pi/2$ , Eqs. (32) simplify to

$$\hat{X} = -\cos \iota \sin \Phi \hat{x} - \cos \iota \cos \Phi \hat{y} + \sin \iota \hat{z}, \quad (34a)$$

$$\hat{Y} = \cos \Phi \hat{x} - \sin \Phi \hat{y}, \quad (34b)$$

$$\hat{Z} = \sin \iota \sin \Phi \hat{x} + \sin \iota \cos \Phi \hat{y} + \cos \iota \hat{z}. \quad (34c)$$

The inverse transformation (33) simplifies to

$$\hat{x} = -\cos \iota \sin \Phi \hat{X} + \cos \Phi \hat{Y} + \sin \iota \sin \Phi \hat{Z}, \quad (35a)$$

$$\hat{y} = -\cos \iota \cos \Phi \hat{X} - \sin \Phi \hat{Y} + \sin \iota \cos \Phi \hat{Z}, \quad (35b)$$

$$\hat{z} = \sin \iota \hat{X} + \cos \iota \hat{Z}. \quad (35c)$$

## 2. From NR-frame to wave-frame

Equations (32) and (34) are of particular importance. By definition, the source-frame basis-vectors are trivially related to vectorial quantities of the CBC dynamics:

$$\hat{x}^{\text{ref}} \equiv \hat{n}, \quad (36a)$$

$$\hat{y}^{\text{ref}} \equiv (\hat{L} \times \hat{n}), \quad (36b)$$

$$\hat{z}^{\text{ref}} \equiv \hat{L}. \quad (36c)$$

Therefore, if the dynamics vectors  $\hat{L}$  and  $\hat{n}$  are known in any coordinate system —e.g., the NR coordinates— then Eqs. (32) yield the wave-frame basis-vectors in those coordinates. Specifically, for  $\Omega = \pi/2$ , Eqs. (34) yield

$$\hat{X}^{\text{ref}} \equiv -\cos i [\sin \Phi \hat{n} + \cos \Phi \hat{L} \times \hat{n}] + \sin i \hat{L}, \quad (37a)$$

$$\hat{Y}^{\text{ref}} \equiv \cos \Phi \hat{n} - \sin \Phi \hat{L} \times \hat{n}, \quad (37b)$$

$$\hat{Z}^{\text{ref}} \equiv \sin i [\sin \Phi \hat{n} + \cos \Phi \hat{L} \times \hat{n}] + \cos i \hat{L}. \quad (37c)$$

Let us consider next the transformation of the GW strain polarizations from the generic (NR) frame Eq. (14) to the wave-frame.  $\hat{X}$  and  $\hat{Y}$  are orthogonal to the direction of propagation  $\hat{Z} = \hat{r}$  of the gravitational wave. Therefore,  $(\hat{\theta}, \hat{\phi})$  can be rotated into  $(\hat{X}, \hat{Y})$  through a rotation by an angle  $\alpha$ :

$$\hat{X} = \cos \alpha \hat{\theta} - \sin \alpha \hat{\phi}, \quad (38a)$$

$$\hat{Y} = \sin \alpha \hat{\theta} + \cos \alpha \hat{\phi}. \quad (38b)$$

Substituting Eqs. (38) into Eqs. (25) we can compute  $h_+^{\text{W}}$  and  $h_{\times}^{\text{W}}$  in terms of  $(\hat{\theta}, \hat{\phi})$ . Comparing further with Eqs. (15), we find:

$$h_+^{\text{W}}(t_{\text{GW}}) = \cos(2\alpha) h_+^{\text{NR}}(t_{\text{GW}}) - \sin(2\alpha) h_{\times}^{\text{NR}}(t_{\text{GW}}), \quad (39a)$$

$$h_{\times}^{\text{W}}(t_{\text{GW}}) = \sin(2\alpha) h_+^{\text{NR}}(t_{\text{GW}}) + \cos(2\alpha) h_{\times}^{\text{NR}}(t_{\text{GW}}). \quad (39b)$$

Not surprising, the GW polarizations in the wave-frame are obtained from those in the NR-frame by a rotation of  $2\alpha$ .

The wave-frame  $\hat{X}, \hat{Y}$  depend on  $\Omega$ , and therefore  $h_+^{\text{W}}$  and  $h_{\times}^{\text{W}}$  also depend on  $\Omega$ . We can make this dependence explicit by resorting to the intermediate vectors  $\hat{P}$  and  $\hat{Q}$ . These are also orthogonal to  $\hat{Z}$ , therefore they, too, can be obtained from  $\hat{\theta}$  and  $\hat{\phi}$  by a rotation:

$$\hat{P} = \cos \alpha' \hat{\theta} - \sin \alpha' \hat{\phi}, \quad (40a)$$

$$\hat{Q} = \sin \alpha' \hat{\theta} + \cos \alpha' \hat{\phi}. \quad (40b)$$

However,  $\hat{P}$  and  $\hat{Q}$  are independent of  $\Omega$  and therefore,  $\alpha'$  is independent of  $\Omega$ . Because  $(\hat{X}, \hat{Y})$  are rotated by  $\Omega$  relative to  $(\hat{P}, \hat{Q})$ , we have

$$\alpha = \Omega + \alpha'. \quad (41)$$

Because rotations add, we can therefore write

$$\begin{pmatrix} h_+^{\text{W}} \\ h_{\times}^{\text{W}} \end{pmatrix} = \mathbf{R}_{2\Omega} \mathbf{R}_{2\alpha'} \begin{pmatrix} h_+^{\text{NR}} \\ h_{\times}^{\text{NR}} \end{pmatrix}, \quad (42)$$

where  $\mathbf{R}_{\beta}$  denotes a 2x2 rotation matrix,

$$\mathbf{R}_{\beta} = \begin{pmatrix} \cos \beta & -\sin \beta \\ \sin \beta & \cos \beta \end{pmatrix}. \quad (43)$$

Equation (42) thus implies that the waveform-modes are obtained from the NR-polarizations by (i) applying an  $\Omega$ -independent rotation by  $2\alpha'$ ; followed by (ii) a rotation by  $2\Omega$ .

For  $\Omega = \pi/2$ , we have  $\mathbf{R}_{\pi} = -\mathbf{1}$ . Therefore, between  $\Omega = 0$  [inclination rotated about X-axis] and  $\Omega = \pi/2$  [inclination rotated about Y-axis], the waveform polarization pick up precisely an overall minus-sign.

### C. Computing GW polarizations in the LAL wave-frame

Let us finally write down explicit instructions of how to obtain GW polarizations in LAL convention, given NR waveform data. Given parameters `i`, `phiRef` passed into `XLALSimInspiralChooseTDWaveform`, proceed as follows:

1. Define  $\Phi = \text{phiRef}$ ,  $t = i$ .
2. Compute  $\hat{Z}_{\text{ref}}$  at the reference time by evaluating Eq. (37c).
3. Because  $\hat{Z}$  points in the direction of emission of the gravitational wave, we must have

$$\hat{Z}_{\text{ref}}^{\text{ref}} \equiv \begin{pmatrix} \cos \phi \sin \theta \\ \sin \phi \sin \theta \\ \cos \theta \end{pmatrix}. \quad (44)$$

From this equality, read off  $(\theta, \phi)$ . Then compute the NR-basis vectors  $\hat{\theta}, \hat{\phi}$  from Eqs. (14).

4. If  $\Omega = \pi/2$ , compute  $\sin \alpha$  and  $\cos \alpha$  by taking inner products of Eq. (38b) with  $\hat{\theta}$  and  $\hat{\phi}$ :

$$\sin \alpha = \cos \Phi \hat{n} \cdot \hat{\theta} - \sin \Phi (\hat{L} \times \hat{n}) \cdot \hat{\theta}, \quad (45a)$$

$$\cos \alpha = \cos \Phi \hat{n} \cdot \hat{\phi} - \sin \Phi (\hat{L} \times \hat{n}) \cdot \hat{\phi}. \quad (45b)$$

If  $\Omega \neq \pi/2$ , compute instead inner products based on Eqs. (32).

5. Substitute  $(\theta, \phi)$  into Eqs. (16) and (15) to compute  $h_+^{\text{NR}}(t_{\text{GW}})$  and  $h_{\times}^{\text{NR}}(t_{\text{GW}})$ .
6. Compute  $\cos 2\alpha = \cos^2 \alpha - \sin^2 \alpha$  and  $\sin 2\alpha = 2 \cos \alpha \sin \alpha$ . Substitute into Eqs. (39) to compute  $h_+^{\text{W}}(t_{\text{GW}})$  and  $h_{\times}^{\text{W}}(t_{\text{GW}})$ .

#### 1. Evaluate spin-consistency in LAL source-frame

The parameters `S1x`, `S1y`, `S1z`, `S2x`, `S2y`, `S2z` passed into `LALSimInspiralChooseTDwaveform` are supposed to be the LAL source-frame parameters, i.e. these parameters should simply be the projections of  $\vec{\chi}_{1,2}$  onto the source-frame basis-vectors  $(\hat{x}, \hat{y}, \hat{z})$ . Substituting Eqs. (22) and (23), one arrives at the following consistency conditions:

$$S1x \stackrel{\text{ref}}{=} \vec{\chi}_1 \cdot \hat{n}, \quad (46a)$$

$$S1y \stackrel{\text{ref}}{=} \vec{\chi}_1 \cdot (\hat{L} \times \hat{n}), \quad (46b)$$

$$S1z \stackrel{\text{ref}}{=} \vec{\chi}_1 \cdot \hat{L}. \quad (46c)$$

The conditions for body 2 are obtained by  $1 \leftrightarrow 2$ .

## V. DISCUSSION

With this new infrastructure it is very easy and much less memory intensive to use NR waveforms directly for data-analysis applications. The “NR\_hdf5” approximant works much the same as any other approximant in `lalsimulation`, but there are a few important differences. The user must supply the location of the HDF5 file, a functionality which was already implemented for NINJA, but was not previously used in `lalsimulation`. Secondly, the user must be careful to supply the mass ratio and spin values that are consistent with the NR files, and the spin values have to be specified in the LAL source frame (see Eqn. (46)).

The current implementation still suffers from a few caveats and drawbacks. As opposed to the continuous waveform approximants, at the moment the metadata are only referring to the beginning of the waveform and not some reference time, which can be chosen freely. While this is not a problem for aligned-spin binaries, this is a big concern for precessing simulations since various quantities, in particular the spins and the orbital angular momentum, are time-dependent. To fully integrate this desired freedom, additional information needs to be incorporated into the HDF5 files and the waveform generator functions accordingly. In the future, we plan to include the frequency evolution of the spins and the orbital angular momentum.

### Acknowledgements

We thank Kent Blackburn for carefully reading through the manuscript and providing useful comments. Many thanks for discussions regarding the frame coordinate transformations to Stas Babak, Jolien Creighton, Michael Pürrer and Ricardo Sturani.

- 
- [1] B. P. Abbott et al. (Virgo, LIGO Scientific), Phys. Rev. Lett. **116**, 061102 (2016), 1602.03837.
  - [2] L. Blanchet, Living Reviews in Relativity **17** (2014), URL <http://www.livingreviews.org/lrr-2014-2>.
  - [3] J. Centrella, J. G. Baker, B. J. Kelly, and J. R. van Meter, Rev. Mod. Phys. **82**, 3069 (2010), 1010.5260.
  - [4] S. Khan, S. Husa, M. Hannam, F. Ohme, M. Pürrer, X. Jimnez Forteza, and A. Boh, Phys. Rev. **D93**, 044007 (2016), 1508.07253.
  - [5] A. Taracchini et al., Phys. Rev. **D89**, 061502 (2014), 1311.2544.
  - [6] J. Healy, C. O. Lousto, and Y. Zlochower, Phys. Rev. **D90**, 104004 (2014), 1406.7295.
  - [7] B. Aylott et al., Class. Quant. Grav. **26**, 165008 (2009), 0901.4399.
  - [8] J. Aasi et al. (VIRGO, LIGO Scientific, NINJA-2), Class. Quant. Grav. **31**, 115004 (2014), 1401.0939.
  - [9] C. R. Galley and P. Schmidt, in prep. (2016), URL <https://dcc.ligo.org/LIGO-P1600064>.
  - [10] C. R. Galley, *romSpline*, URL <https://bitbucket.org/chadgalley/romspline>.
  - [11] D. Brown, S. Fairhurst, B. Krishnan, R. A. Mercer, R. K. Koppurapu, L. Santamaria, and J. T. Whelan (2007), 0709.0093.
  - [12] T. Dal Canton et al., Phys. Rev. **D90**, 082004 (2014), 1405.6731.
  - [13] A. H. Mroue et al., Phys. Rev. Lett. **111**, 241104 (2013), 1304.6077.
  - [14] M. Boyle and A. H. Mroue, Phys. Rev. **D80**, 124045 (2009), 0905.3177.
  - [15] The customary choice of many NR groups is to *start* NR simulations with  $\hat{L} = \hat{e}_z$ . Because of junk-radiation and precession effects,  $\hat{L}(t)$  will deviate from  $\hat{e}_z$ . This deviation generally will be very small for aligned-spin BBH systems, but may become significant for precessing systems.